ACS APPLIED MATERIALS & INTERFACES

Research Article

Cite This: ACS Appl. Mater. Interfaces 2019, 11, 37130−37138

www.acsami.org

Gradient Assembly of Polymer Nanospheres and Graphene Oxide Sheets for Dual-Responsive Soft Actuators

Yuan-Yuan Gao,[†] Yong-Lai Zhang,*[,†] Bing Han,[‡] Lin Zhu,[†] Biao Dong,[†] and Hong-Bo Sun*[,‡]

[†]State Key Laboratory of Integrated Optoelectronics, College of Electronic Science and Engineering, Jilin University, 2699 Qianjin Street, Changchun 130012, China

[‡]State Key Laboratory of Precision Measurement Technology & Instruments, Department of Precision Instrument, Tsinghua University, Haidian District, Beijing 100084, China

Supporting Information

ABSTRACT: Bimorph actuators hold great promise for developing soft robots. However, poor interlayer adhesion between different materials always threatens their stability for long-term usage. In this paper, instead of using a bilayer structure, we reported the gradient assembly of graphene oxide (GO) sheets and polymer nanospheres for developing robust moisture and light dual-responsive actuators. The distribution gradient of poly(methyl methacrylate) (PMMA) nanospheres along the normal direction of a GO paper leads to an asymmetric structure. The front side that mainly consists of GO is quite sensitive to water molecules, which swells upon exposure to moisture, whereas the back side that is rich in PMMA nanospheres expands obviously due to the photothermal effect. The distinct properties of the two sides endow the composite paper with moisture and light dual-responsiveness. Moreover, since GO has been used as a host material, the composite paper shows a moisture-triggered self-healing property, which permits front-to-front and front-to-back healing. The self-healed paper can maintain similar responsive property and reasonable mechanical strength to the pristine one. As a proof of concept, a dual-responsive gripper actuator and a scorpion robot have been fabricated for light and moisture cooperative manipulation. The gradient assembly strategy may open up a new way for developing robust multiresponsive actuators beyond bilayer structures.

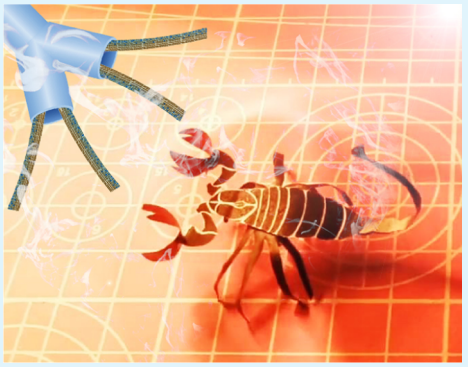

KEYWORDS: *graphene oxide, polymer nanospheres, dual-response, actuators, soft robots*

INTRODUCTION

Bimorph actuators that can convert environmental stimuli to mechanical work by deforming themselves are very promising for soft robotics.[1−3] A general concept for developing bimorph actuators is using bilayer structures based on two different materials of distinct properties. Under a certain external stimulation, for instance temperature,[4−6] light,[7] moisture,[8,9] pH,[10,11] and chemical reagents,[12] one layer may undergo more obvious volume change (swelling or shrinking) than the other layer.[13−15] In this way, a strain mismatch occurs at the bimaterial interface, causing the deformation of the bilayer structure. Based on this simple design principle, various bimorph actuators have been successfully developed using different materials.[7,9,15−18] For instance, bilayer materials with distinct thermal expansion coefficients (TECs) can be actuated by temperature change;[19−21] the integration of moisture-responsive hydrogels with hydrophobic polymers can lead to moisture-responsive bimorph actuators;[22,23] photothermal/electrothermal materials can be combined with temperature-sensitive bilayers for developing light/electric-driven actuators.[24−26] To date, although bimorph actuators have proven it value in both fundamental science and practical applications, continued efforts in developing novel stimuli-responsive materials are still highly desired to achieve fast response, multiform actuation, larger scale deformation and long-term stability.[27]

Recently, graphene oxide (GO), a natural two-dimensional material, has been widely employed for developing bimorph actuators.[28,29] Typically, GO has revealed several distinct advantages.[30] First, GO sheets that possess abundant oxygen containing groups (OCGs) show strong interaction with water molecules. Unlike pristine graphene that interacts with water molecules through relatively weak van der Waals force, the OCGs on GO and water molecules can form much stronger hydrogen bonds. The adsorption and desorption of water molecules can lead to ultrafast and reversible swelling and shrinking of the GO layer.[31] Thus, GO can be combined with moisture-inert materials for moisture-responsive actuators.[8,32,33] Second, GO permits the modification of OCGs through different chemical/physical routes and thus its moisture-responsive property can be tuned in a highly controlled manner. For instance, Qu et al. reported a very impressive moisture-responsive fiber, which is prepared by femtosecond laser selective modification of a GO fiber.[34] In

Received: July 29, 2019
Accepted: September 10, 2019
Published: September 10, 2019

DOI: 10.1021/acsami.9b13412
ACS Appl. Mater. Interfaces 2019, 11, 37130−37138

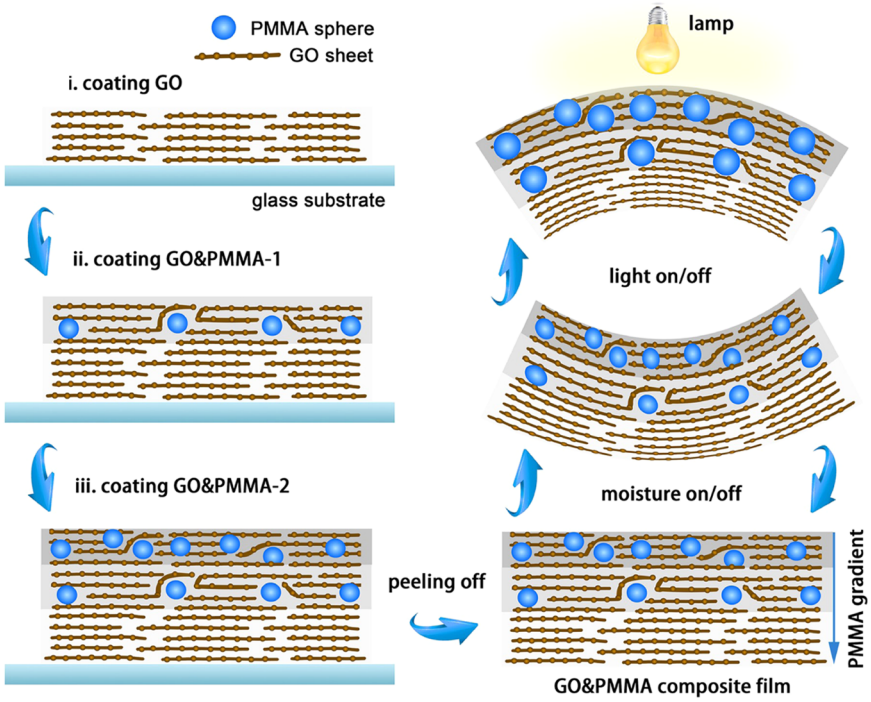

Figure 1. Schematic illustration for the preparation (left column, gradient assembly of GO sheets and PMMA nanospheres) and moisture/light actuation (right column) of the GO/PMMA nanosphere composite paper.

our previous work, we have reported a self-controlled photoreduction strategy for fabricating smart GO/reduced GO bilayers as moisture actuators.[8] Third, GO-based actuators permit multiform actuation.[30] For instance, light irradiation can promote the desorption of water molecules, leading to volume shrinking.[35] Selective reduction of GO can render its conductivity, thus enabling electrothermal actuation.[36] Moreover, GO possesses a very small or even negative TEC. Therefore, under thermal/photothermal/electrothermal actuation, it can act as a temperature-inert layer and cause much obvious strain mismatch.[7] In the past five years, serving as a versatile material, GO has proven its value in various bimorph actuators.[37] However, in combination with other functional materials, GO usually shows relatively weak interlayer interaction, resulting in poor stability. The GO film prepared by spin coating or drop coating is a natural layered structure. GO sheets interact with each other through relatively strong hydrogen bonds; whereas the entire GO film interacts with other materials generally through relatively weak van der Waals force. As a result, bimorph actuators based on GO and other materials may suffer from poor interlayer stability in long-term usage. The stimuli induced interlayer strain mismatch can cause detachment of the bilayers during frequent bending−unbending deformation. This drawback significantly limits the practical applications of GO-based bimorph actuators.

In this paper, we reported an alternative route for fabricating GO-based actuators. Instead of forming a bilayer structure, we doped GO with poly(methyl methacrylate) (PMMA) nanospheres and controlled the distribution gradient of the PMMA nanospheres along the normal direction of the paper through a sequential assembly process. The resultant GO/PMMA nanosphere composite paper exhibits an asymmetric structure, where one side is composed of GO and the other side is rich in PMMA nanospheres. The composite paper permits moisture and light dual-stimuli actuation and reveals fast response/recovery time. More importantly, without an obvious two-material interface, the composite paper shows good stability for long-term usage and enables self-healing under moisture treatment. The robust GO/PMMA nanosphere composite paper has been employed to fabricate moisture and light dual-responsive smart devices, including a gripper and a scorpion robot.

EXPERIMENTAL METHODS

Preparation of PMMA Nanospheres. The PMMA nanospheres (~500 nm in diameter) used in this study were synthesized according to a reported literature.[38] In our experiment, 0.6 g of PMMA nanosphere powder was dispersed in 1 mL of deionized water under magnetic stirring for 5 h until the solution turns uniform white.

Preparation of GO@PMMA-1 and GO@PMMA-2 Aqueous Solutions. GO was prepared via an improved Hummer's method using natural graphite powder (Aldrich, <150 μm) as the raw material. To remove the residual ions, the GO aqueous solution was washed with pure water several times until the solution becomes neutral. The GO@PMMA-1 and GO@PMMA-2 aqueous solutions with different PMMA contents were prepared by mixing 30 μL of the above-mentioned PMMA solution with 50 or 20 mL of GO solution, respectively (Figure S1, supporting information). The mixture was stirred for at least 1 h to ensure that the PMMA nanospheres were incorporated homogeneously onto the GO sheets by electrostatic force.

Preparation of GO/PMMA Nanosphere Composite Paper. The GO/PMMA nanosphere composite paper was prepared through sequential assembly of GO, GO−PMMA-1, and GO−PMMA-2 aqueous solutions. Typically, 10 mL of GO aqueous solution was casted on a glass substrate and dried in ambient conditions. Then, 5 mL of GO−PMMA-1 aqueous solution was casted on the GO surface. After drying in ambient conditions, 5 mL of GO−PMMA-2 was casted on the surface and dried in ambient conditions. Finally, the GO/PMMA nanosphere composite paper with PMMA nanosphere gradient formed, which was peeled from the glass substrate for further usage.

DOI: 10.1021/acsami.9b13412
ACS Appl. Mater. Interfaces 2019, 11, 37130−37138

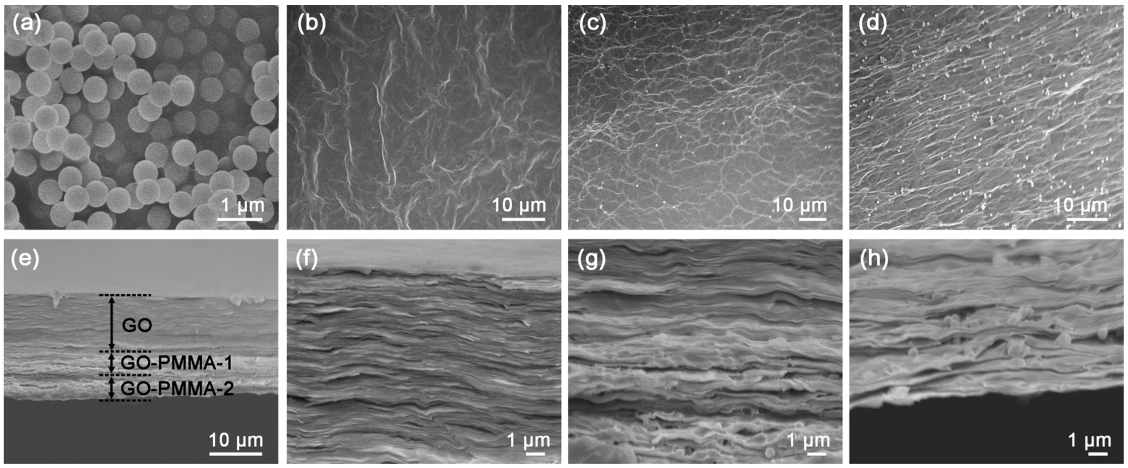

Figure 2. SEM images of the (a) PMMA nanospheres, (b) GO film surface, (c) GO−PMMA-1 surface, and (d) GO−PMMA-2 surface; section-view SEM images of the (e) GO and PMMA nanosphere composite paper, (f) GO region, (g) GO−PMMA-1 region, and (h) GO−PMMA-2 region.

Fabrication of a Dual-Responsive Gripper and Scorpion Robot. A dual-responsive gripper was fabricated by integrating two pairs of GO/PMMA composite ribbons with a "Y"-shaped plastic tube. With the help of four small pieces of double-sided tape, the four ribbons (1 × 10 mm^2) were pasted onto the inner wall of the tube with the GO side facing each other. For the fabrication of the scorpion robot, a paper body of the scorpion pattern was printed, cut, and used. Then, two claws, four pairs of legs, and a long tail were cut from the GO/PMMA nanosphere composite paper according to a prepatterned template. The claws, legs, and tail were pasted onto the paper body using small pieces of double-sided tape.

Characterization. The SEM images of the samples were obtained using a JEOL JSM-7500F field-emission scanning electron microscope. X-ray photoelectron spectroscopy (XPS) was performed using an ESCALAB 250 spectrometer (Thermo Fisher Scientific).[39] Powder X-ray diffraction (XRD) patterns were collected on a Rigaku D/MAX 2550 diffractometer with Cu Kα radiation (λ = 1.5418 Å). Raman spectra were measured on JOBIN YVON T64000 equipped with a liquid-nitrogen-cooled argon ion laser at 532 nm (Spectra-Physics Stabilite 2017) as an excitation source. IR spectroscopy was recorded using an FT-IR Nicolet 5700 spectrometer in the 4000−400 cm^{-1} frequency range, using powdered samples diluted in KBr pellets. The controlled humidity environments were achieved using saturated aqueous solutions of LiCl, CH_3COOK, $MgCl_2$, K_2CO_3, NaBr, KI, NaCl, KCl, and K_2SO_4 in a closed glass vessel at an ambient temperature of 25 °C,[40] which yielded approximately 11, 23, 33, 43 59, 69.9, 75, 86, and 96% relative humidity (RH), respectively.[41]

RESULTS AND DISCUSSION

Preparation of GO/PMMA Nanosphere Composite Paper. We prepared the GO/PMMA nanosphere composite paper through a gradient assembly method. As shown in Figure 1, GO aqueous solution was first casted on a glass substrate and dried in ambient conditions. A continuous GO film with a layered nanostructure formed after water evaporation. Then, the GO−PMMA-1 solution that contains less amount of PMMA nanospheres was coated on the surface of the GO film. Evaporation-induced self-assembly of the GO sheets and the PMMA nanospheres leads to the formation of a GO and polymer nanosphere composite layer. After that, the GO−PMMA-2 solution containing more PMMA nanospheres was coated. In this way, a GO/PMMA nanosphere composite paper with tailored PMMA nanosphere gradient along the normal direction has been prepared, which was peeled off from the glass substrate for subsequent experiments. Since the composite paper has an asymmetric structure, where one side is composed of GO and the other side is rich in PMMA nanospheres, it demonstrated dual-responsiveness. In response to moisture, the GO side would swell more obviously due to the adsorption of water molecules, leading to bending toward the PMMA side. On the contrary, upon light irradiation, the photothermal effect would promote the desorption of water from the GO side and cause the expansion of PMMA nanospheres on the other side simultaneously. Here, GO has a very small or even negative TEC,[20,21] whereas PMMA has a positive and relatively large TEC. As a result, the paper would bend toward the reverse direction upon photothermal heating. The dual-responsive property makes the GO/PMMA nanosphere composite paper more tractable in moisture and light actuation. In this work, we employed a trilayer structure, in which the GO layer is used as a moisture-active/light-inert layer; the intercomposite layer with less PMMA nanospheres is a transition layer; and the composite layer with more PMMA nanospheres works as a light-active/moisture-inert layer. Actually, to further control the gradient of PMMA nanospheres, using more layers with gradually changed PMMA concentrations is also workable. Nevertheless, to achieve a sensitive response to both moisture and light, the thickness of these layers should be optimized.

Characterization of GO/PMMA Nanosphere Composite Paper. The PMMA nanospheres used in this work is very uniform; the average size is ∼500 nm in diameter (Figure 2a). To investigate the surface morphologies of different layers, we characterized the GO, GO−PMMA-1, and GO−PMMA-2 surfaces, respectively, by scanning electron microscopy (SEM). As shown in Figure 2b, the GO surface shows abundant wrinkles. This is the typical surface morphology of the GO film. After coating with GO−PMMA-1 solution, the numbers of wrinkles increased. Randomly distributed PMMA nanospheres can be identified from the image (Figure 2c). The coating of GO−PMMA-2 solution can further increase the wrinkles due to the presence of more PMMA nanospheres (Figure 2d). To investigate the distribution of PMMA nanospheres along the normal direction, we also get the section-view SEM images of the composite paper. As shown in Figure 2e, the composite paper is about 20 μm in thickness, in which the GO layer is about 10 μm and the GO−PMMA-1 and GO−PMMA-2 layers are both 5 μm. Magnified SEM

DOI: 10.1021/acsami.9b13412
ACS Appl. Mater. Interfaces 2019, 11, 37130−37138

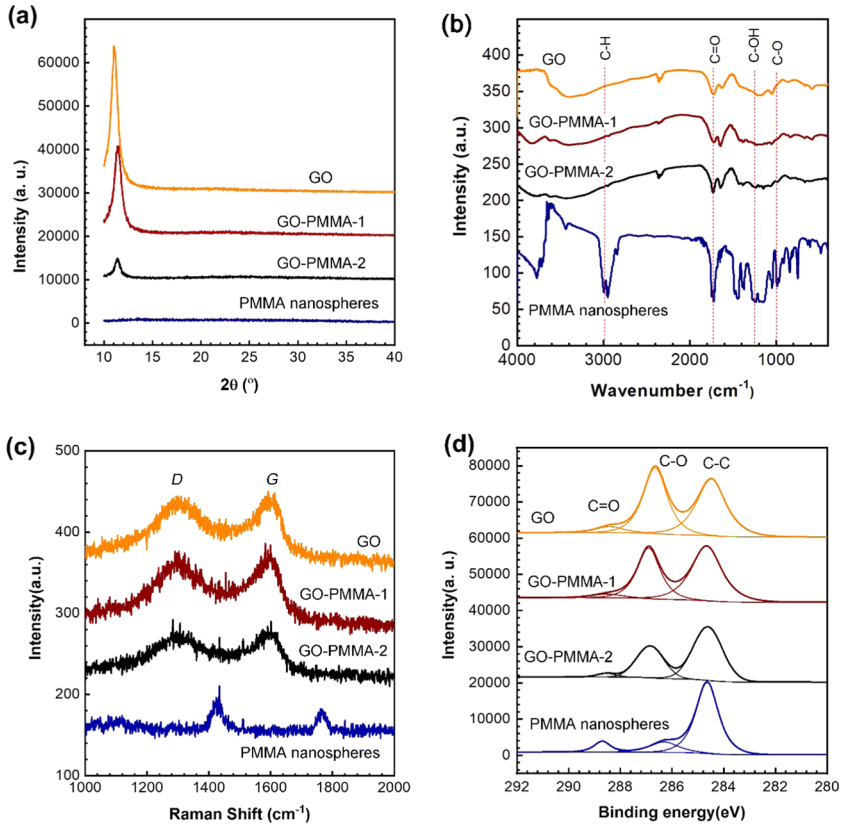

Figure 3. Characterization of PMMA nanospheres, GO, GO−PMMA-1, and GO−PMMA-2 samples: (a) XRD patterns, (b) FT-IR spectra, (c) Raman spectra, and (d) C 1s XPS spectra.

images show that the GO layer has nanolayer structures (Figure 2f), indicating the ordered stacking of GO sheets. At the GO−PMMA-1 region, the ordered degree decreased, and PMMA nanospheres can be observed randomly among the GO layers (Figure 2g). At the GO−PMMA-2 region, the ordered degree further decreased and more PMMA nanospheres can be identified (Figure 2h). Since GO has been used as a host material and only the distribution of PMMA nanospheres have been tuned along the normal direction, no obvious interlayer bounds can be detected.

In addition to the morphologies, we also characterized these samples by X-ray diffraction (XRD, Figure 3a). The XRD patterns of GO show a diffraction peak at 2θ = 11.7°, corresponding to a *d*-spacing of 0.75 nm. In the presence of PMMA nanospheres, the intensity of the diffraction peaks of GO−PMMA-1 and GO−PMMA-2 samples decreased obviously, because the 500 nm PMMA nanospheres make the layered GO structure more disordered. PMMA nanospheres are amorphous, and no diffraction peaks can be detected. FT-IR spectra of these samples show the typical stretching peaks of both GO and PMMA (Figure 3b). Typically, the characteristic absorption peaks of PMMA at 2953 cm^{-1} (2800−3000 cm^{-1}) can be assigned to the C−H stretching vibrations and the strong absorption band at 989 cm^{-1} can be attributed to the C−O stretching of the ester group. The absorption band at 1730 cm^{-1} can be assigned to the C═O stretching vibrations, and a C−OH stretching peak appears at 1230 cm^{-1}. Typical peaks for both PMMA and GO could be simultaneously found in the samples of GO−PMMA-1 and GO−PMMA-2, indicating the presence of GO and PMMA nanospheres. Besides, Raman spectra were employed to characterize these samples. For GO, GO−PMMA-1, and GO−PMMA-2 samples, the D-band peak at 1338 cm^{-1} corresponding to disordered sp^3 carbon and the G-band peak (the E_{2g} mode of graphite) at 1598 cm^{-1} can be observed, indicating the presence of GO. For PMMA nanospheres, the D-band and G-band are absent (Figure 3c).[42]

The C 1s XPS spectra for GO, GO−PMMA-1, and GO−PMMA-2 samples can be deconvoluted into three peaks at 284.6, 286.6, and 288.4 eV. These peaks correspond to nonoxygenated ring carbon (C−C), hydroxyl or epoxy carbon (C−O), and carbonyl carbon (C═O), respectively (Figure 3d). For GO, the content of carbon bonded to carbon was 49%, and more than half of the carbon atoms were bonded to oxygen by forming C−O or C═O. In the case of GO−PMMA-1 and GO−PMMA-2 samples, the contents of the C−C bond increased to 57 and 64%, respectively, due to the presence of PMMA nanospheres.[43] Note that the PMMA nanospheres have a C−C content of 77%. As observed from Figure 3d, the C−O peaks decreased obviously with the increase of PMMA nanosphere contents. The distinct oxygen contents of the two sides (GO and GO−PMMA-2) make the GO/PMMA nanosphere composite paper smart under moisture actuation. Since water molecules would be preferentially adsorbed by the GO side where there are abundant OCGs, bending occurs toward the GO−PMMA-2 side where the OCGs are fewer.

Moisture and Light Response Properties. Owing to its asymmetric structure, the GO/PMMA nanosphere composite paper is very sensitive to both moisture and light. To quantitatively investigate the moisture- and light-responsive properties, we cut the composite paper into a ribbon of 1 × 20

DOI: 10.1021/acsami.9b13412
ACS Appl. Mater. Interfaces 2019, 11, 37130−37138

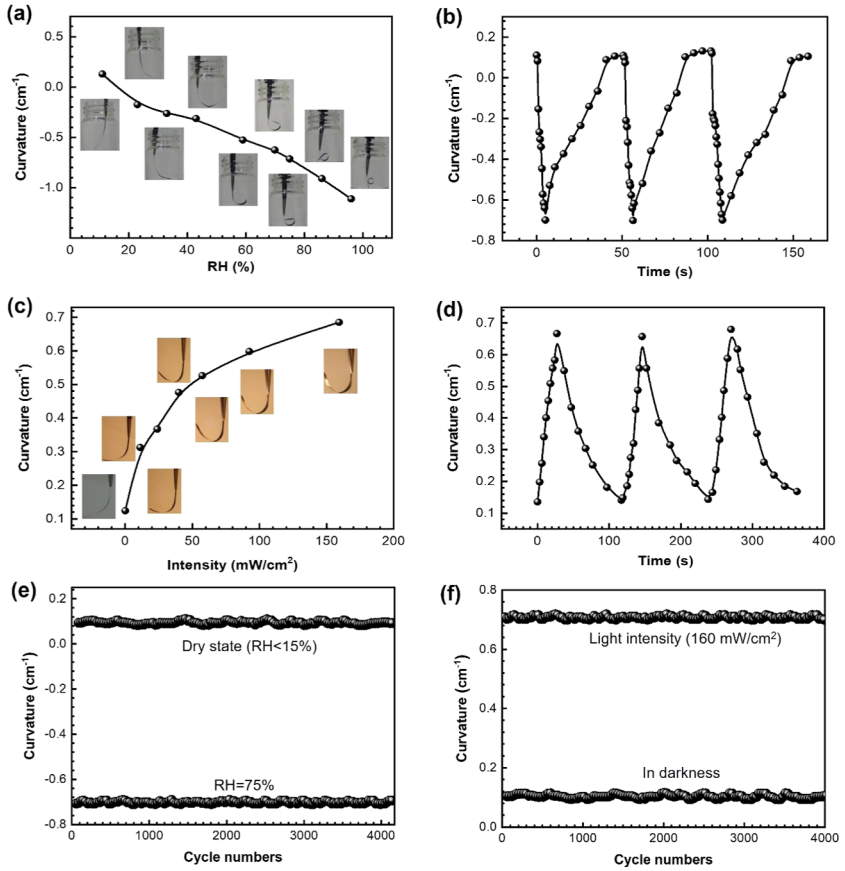

Figure 4. Moisture- and light-responsive properties of the GO/PMMA nanosphere composite paper. (a) Dependence of curvature on relative humidity; (b) moisture response and recover property of the composite paper; (c) dependence of curvature on light intensity; (d) light response and recover property of the composite paper; (e) long-term stability of the moisture-induced deformation, and the humidity was switched between the dry state (RH < 15%) and RH = 75%; (f) long-term stability of the light-driven deformation, where the light intensity was 160 mW/cm^2.

mm^2 size and measured the deformation curvature of the ribbon under different stimuli conditions. Figure 3a shows the dependence of curvature on relative humidity. Here, since the ribbon would bend toward different directions under moisture and light actuation, we defined the bending toward the GO side as the positive curvature. With the increase of RH, the GO/PMMA composite ribbons curve to a higher degree toward the GO−PMMA-2 side through quasilinear dependence. The maximum curvature of ∼−1.1 cm^{-1} was observed when the RH is 97%. The moisture-induced bending deformation is reversible; by switching the RH between the dry state (RH < 15%) and the moisture state (RH = 75%), the bending curvature could be switched freely from ∼0.12 to ∼−0.70 cm^{-1} (Figure 4a). The moisture responsiveness is very fast. The average response time for bending and straightening processes is measured to be 5 and 35 s, respectively (Figure 4b). According to a newly published result,[31] the response and recovery time of moisture-triggered GO actuators can be improved by introducing nanostructures in the GO layer.

The GO/PMMA nanosphere composite paper can also be actuated by light. Under light illumination, GO can absorb the photoenergy and convert it to heat, which causes the increase of local temperature. For one hand, the temperature rise can promote the desorption of water molecules; for the other hand, the photothermal effect would increase the volume of PMMA nanospheres since PMMA possesses a positive TEC. The synergistic effect (photothermal desorption of water with respect to the GO side and the photothermal expansion of the PMMA side) leads to the deformation of the composite ribbon toward the opposite side. With the increase of light intensity, the ribbon bent toward the higher curvature. The maximum curvature of ∼0.65 cm^{-1} was observed when the light intensity is ∼160 mW/cm^2. The light actuation is also reversible. By switching on and off the light, the bending curvature could be tuned from ∼0.12 to ∼0.65 cm^{-1} (Figure 4c). The response and recovery time for bending and straightening processes are 27 and 90 s, respectively (Figure 4d). As compared with the state-of-the-art GO-based photothermal actuators,[25] the light responsiveness is not the fastest one. To achieve a much faster response, photothermal materials, such as Au nanorods,[7] can be combined with the composites.

More importantly, the GO/PMMA nanosphere composite paper shows excellent stability for cycling deformation under moisture and light actuation. After switching the RH between the dry state (RH < 15%) and moisture state (RH = 75%) for 4000 cycles, the actuator shows a very stable deformation degree; the curvatures at different states are almost constant values (Figure 4e). Similar to moisture actuation, the actuator also demonstrates stable light-driven deformation for 4000 cycles (Figure 4f), indicating its robustness for long-term usage.

Self-healing Properties of GO/PMMA Nanosphere Composite Paper. Since GO has been employed as the host material, the composite paper shows moisture-triggered self-healing properties. As shown in Figure 5a, a piece of GO/PMMA composite paper was cut into two pieces, both with

DOI: 10.1021/acsami.9b13412
ACS Appl. Mater. Interfaces 2019, 11, 37130−37138

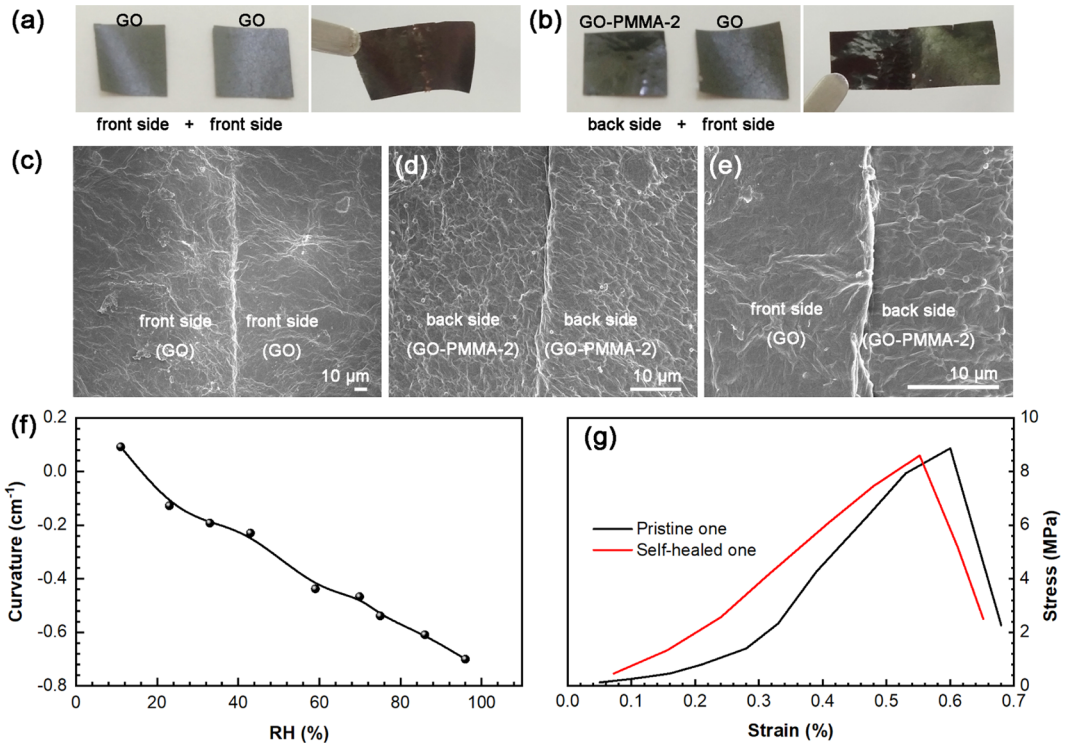

Figure 5. Moisture-triggered self-healing properties of the GO and PMMA nanosphere composite paper. (a) Photographs of a pair of GO and PMMA nanosphere composite papers with GO as the front side; the right photograph shows the front-to-front self-healed composite paper; (b) photographs of a pair of GO and PMMA nanosphere composite papers with GO and GO−PMMA-2 as the front sides, respectively; the right photograph shows the front-to-back self-healed composite paper; (c) SEM image of the front-to-front self-healed region at the GO side; (d) SEM image of the front-to-front self-healed region at the back side (GO−PMMA-2); (e) SEM image of the front-to-back self-healed region; (f) moisture-responsive property of the front-to-front healed composite paper; (g) mechanical strength of the pristine composite paper and the self-healed composite paper.

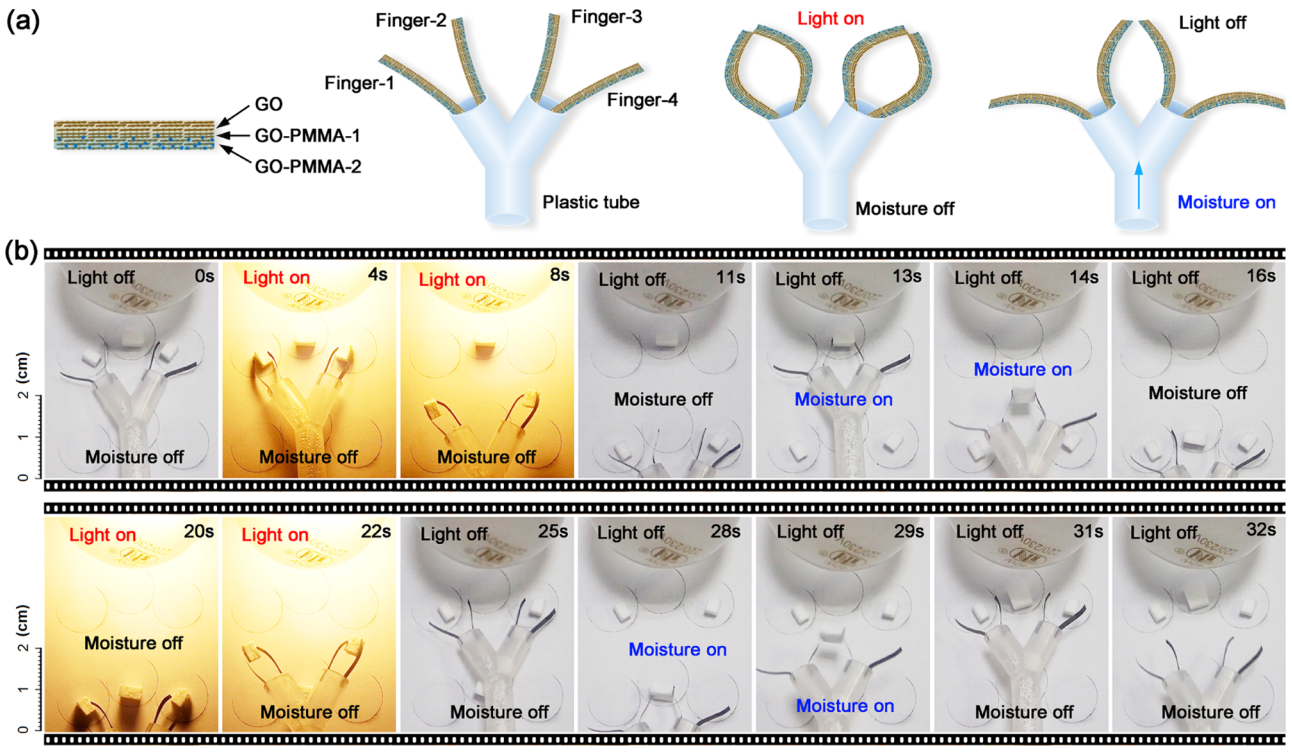

Figure 6. Moisture and light dual-responsive gripper actuator. (a) Schematic illustration of the structure and the deformation of the dual-responsive gripper actuator; (b) moisture- and light-cooperative manipulation of the dual-responsive gripper actuator.

DOI: 10.1021/acsami.9b13412
ACS Appl. Mater. Interfaces 2019, 11, 37130−37138

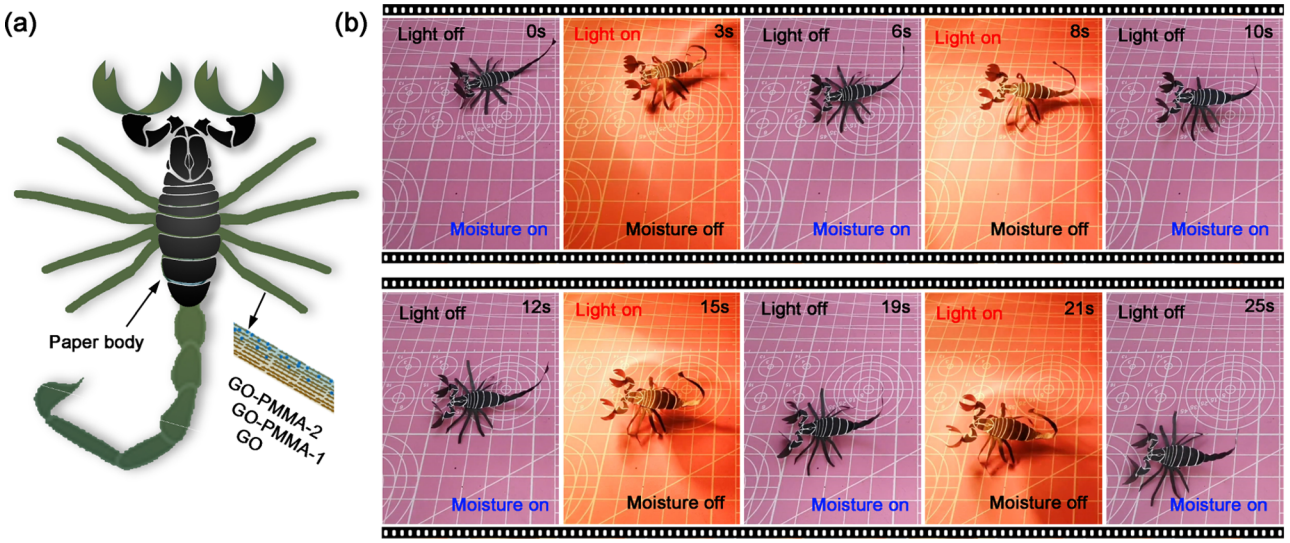

Figure 7. Moisture and light dual-responsive scorpion robot. (a) Schematic illustration of the structure of the dual-responsive scorpion robot; (b) moisture- and light-cooperative manipulation of the dual-responsive scorpion robot. The scale bar for one square is 1 cm.

GO as the front side. The two pieces can be cured together after moisture treatment for several seconds and dried in ambient conditions. In addition to the front-to-front self-healing, the two pieces of composite paper can be healed in a front-to-back manner (Figure 5b). SEM images of the self-healed region shows the local structure change after self-healing. As observed from the front side (GO side), a rough ridge can be observed at the cut (Figure 5c). The moisture-induced self-healing process can be considered as the reassembly of the GO nanosheets. On the other side, the GO−PMMA-2 surface can also be cured (Figure 5d). Here, the reassembly of GO plays a critical role in self-healing. Therefore, in the case of front-to-back self-healing, the two pieces can be easily integrated through the same manner (Figure 5e). Since the deformation of the GO/PMMA composite paper is predictable, front-to-back healing of the composite paper may form new actuators that enable more complex deformation. To evaluate the cured GO/PMMA nanosphere composite paper, we tested both the moisture-responsive deformation performance and the mechanical strength. As shown in Figure 5f, the self-healed composite paper can maintain a similar deformation degree to the pristine one. In the mechanical test, the breaking stress of the self-healed composite paper decreased only slightly as compared with the pristine one, indicating its good mechanical strength (Figure 5g). For actuators, the self-healing properties are quite important for promoting their robustness, especially for practical applications. Moreover, the self-healing properties make it possible to be integrated in separated actuators flexibly, which can facilitate the fabrication of soft robots.

Moisture and Light Dual-Responsive Actuators. As a proof of concept, we fabricated two kinds of actuators for moisture- and light-cooperative manipulation. Figure 6 shows the moisture and light dual-responsive gripper. We integrated two pairs of GO/PMMA nanosphere composite ribbons (Finger-1−Finger-4) with a Y-shaped plastic tube that is connected to moisture (Figure 6a). For each channel, a pair of fingers was attached with the GO side facing each other. In this way, the two pairs of fingers can functionalize as two grippers under light actuation. In response to moisture, Finger-2 and Finger-3 would bend toward the opposite side and functionalize as a new gripper. To test the real performance of this dual-responsive gripper, we demonstrate its picking-up and releasing functions in the transport of three polymer foam blocks. Figure 6b shows the snapshots of the manipulation procedure. Under light irradiation, the two pairs of fingers can pick up the left and right blocks. When we turned off the light, the two blocks can be released at the bottom position. After that, moisture was supplied and Finger-2 and Finger-3 picked up the middle block and released it after turning off the moisture. By repeating the above process, the smart gripper can transport these blocks back to the original positions (Video S1).

As a photothermal actuator, temperature also plays a critical role in moisture and light actuation. In this work, we fixed the environmental temperature at a constant value and controlled the humidity-induced deformation by providing moisture intermittently. If the humidity gradient could be well controlled near the actuators, more precise manipulation would be realized. For light actuation, GO has broad adsorptions throughout the UV and visible-light range (Figure S2). Consequently, various light sources can be used for actuation. Nevertheless, considering UV reduction of GO, visible and near-IR light sources, such as filament lamp, are good choices.

Figure 7 demonstrates the manipulation of a scorpion robot. In this work, the body of the scorpion was made of general paper, as shown in the black region of Figure 7a. The two claws, the four pairs of legs, and the long tail are made of GO/PMMA nanosphere composite paper (GO−PMMA-2 as the front side). The total size of the scorpion is about 4.5 cm in width. We control this moisture-responsive scorpion robot using a self-made moisture-supplying system (Figure S3). Upon exposure to moisture, the scorpion robot sprawled on the ground. Under light irradiation, the scorpion stood up, its claws closed, and its tail curled up. By switching these two actuation processes, the scorpion can walk downside gradually, since its gravity center changed during the deformation of the legs and the tail. Within 25 s, we have switched the moisture and light four times and the scorpion walked ∼5 cm (Figure 7b, Video S2).

DOI: 10.1021/acsami.9b13412
ACS Appl. Mater. Interfaces 2019, 11, 37130−37138

CONCLUSIONS

In conclusion, dual-responsive graphene actuators have been successfully fabricated by sequential assembly of GO and PMMA aqueous solutions. By controlling the distribution and amount of the PMMA nanospheres, the gradient of PMMA nanospheres could be continuously tuned along the normal direction of the composite paper. Instead of a general bilayer structure, an asymmetric gradient structure formed, one side is composed of GO and the other side is rich in PMMA nanospheres. Due to the presence of abundant OCGs on the GO sheets, the asymmetric composite paper demonstrated much better water adsorption capacity on the GO side and thus bent toward the PMMA nanosphere-rich side in response to moisture. Under light actuation, the photothermal effect induced water molecule desorption and the thermal expansion of PMMA nanospheres caused the mismatch of strain from the two sides, and the composite paper bent toward the opposite side. A large-scale bending curvature from −1.1 to 0.65 cm^{-1} has been achieved under moisture and light actuation. Without a bimaterial interface, dual-responsive composite paper exhibits excellent stability for long-term bending/unbending deformation under 4000 moisture- and light-actuation cycles. More importantly, the composite paper shows a moisture-induced self-healing property, which promotes its robustness for practical usage. Using these GO/PMMA nanosphere composite actuators as basic components, dual-responsive paper robots including a gripper and a scorpion robot have been demonstrated.

ASSOCIATED CONTENT

Supporting Information

The Supporting Information is available free of charge on the ACS Publications website at DOI: 10.1021/acsami.9b13412.

Photographs of GO, PMMA nanospheres, GO−PMMA-1, and GO−PMMA-2 aqueous solutions; absorption spectrum of GO aqueous solution and the schematic illustration of the self-made moisture-supplying system (PDF)

Moisture- and light-cooperative manipulation of the gripper (MP4)

Moisture- and light-cooperative manipulation of the scorpion robot (AVI)

AUTHOR INFORMATION

Corresponding Authors

*E-mail: yonglaizhang@jlu.edu.cn (Y.-L.Z.).
*E-mail: hbsun@tsinghua.edu.cn (H.-B.S.).

ORCID

Yong-Lai Zhang: 0000-0002-4282-250X
Hong-Bo Sun: 0000-0003-2127-8610

Present Address

§If an author's address is different from the one given in the affiliation line, this information may be included here.

Author Contributions

The manuscript was written through contributions of all authors. All authors have given approval to the final version of the manuscript.

Notes

The authors declare no competing financial interest.

ACKNOWLEDGMENTS

The authors acknowledge the National Key Research and Development Program of China and the National Natural Science Foundation of China under Grant Nos. 2017YFB1104300, 61935008, 61775078, 61590930, and 61605055 for support. We also acknowledge the Natural Science Foundation of Jilin Province under Grant No. 20180101061JC.

REFERENCES

(1) Xu, G.; Zhang, M.; Zhou, Q.; Chen, H.; Gao, T.; Li, C.; Shi, G. A Small Graphene Oxide Sheet/Polyvinylidene Fluoride Bilayer Actuator with Large and Rapid Responses to Multiple Stimuli. *Nanoscale* **2017**, *9*, 17465−17470.

(2) Zakaria, M. B.; Li, C.; Ji, Q.; Jiang, B.; Tominaka, S.; Ide, Y.; Hill, J. P.; Ariga, K.; Yamauchi, Y. Self-Construction from 2D to 3D: One-Pot Layer-by-Layer Assembly of Graphene Oxide Sheets Held Together by Coordination Polymers. *Angew. Chem., Int. Ed.* **2016**, *55*, 8426−8430.

(3) Zhao, F.; Zhao, Y.; Chen, N.; Qu, L. Stimuli-Deformable Graphene Mmaterials: From Nanosheet to Macroscopic Assembly. *Mater. Today* **2016**, *19*, 146−156.

(4) Wasserman, D. Nanosecond Modulation of Thermal Emission. *Light Sci. Appl.* **2019**, *8*, No. 68.

(5) Tang, L.; Gong, L.; Zhou, G.; Liu, L.; Zhang, D.; Tang, J.; Zheng, J. Design of Low Temperature-Responsive Hydrogels Used as A Temperature Indicator. *Polymer* **2019**, *173*, 182−189.

(6) Xie, H.; Li, L.; Cheng, C.-Y.; Yang, K.-K.; Wang, Y.-Z. Poly(ethylene-co-vinyl acetate)/Graphene shape-memory Actuator with A Cyclic Thermal/Light Dual-Sensitive Capacity. *Compos. Sci. Technol.* **2019**, *173*, 41−46.

(7) Han, B.; Zhang, Y.-L.; Zhu, L.; Li, Y.; Ma, Z.-C.; Liu, Y.-Q.; Zhang, X.-L.; Cao, X.-W.; Chen, Q.-D.; Qiu, C.-W.; Sun, H.-B. Plasmonic-Assisted Graphene Oxide Artificial Muscles. *Adv. Mater.* **2019**, *31*, No. 1970029.

(8) Han, D.-D.; Zhang, Y.-L.; Jiang, H.-B.; Xia, H.; Feng, J.; Chen, Q.-D.; Xu, H.-L.; Sun, H.-B. Moisture-Responsive Graphene Paper Prepared by Self-Controlled Photoreduction. *Adv. Mater.* **2015**, *27*, 332−338.

(9) Yang, B.; Bi, W.; Zhong, C.; Huang, M.; Ni, Y.; He, L.; Wu, C. Moisture-Triggered Actuator and Detector with High-Performance: Interface Engineering of Graphene Oxide/Ethyl Cellulose. *Sci. China Mater.* **2018**, *61*, 1291−1296.

(10) Shojaeifard, M.; Bayat, M. R.; Baghani, M. Swelling-Induced Finite Bending of Functionally Graded pH-Responsive Hydrogels: A Semi-Analytical Method. *Appl. Math. Mech.* **2019**, *40*, 679−694.

(11) Strachota, B.; Strachota, A.; Slouf, M.; Brus, J.; Cimrova, V. Monolithic Intercalated PNIPAm/Starch Hydrogels with Very Fast and Extensive One-Way Volume and Swelling Responses to Temperature and pH: Prospective Actuators and Drug Release Systems. *Soft Matter* **2019**, *15*, 752−769.

(12) Zhao, L.; Huang, J.; Zhang, Y.; Wang, T.; Sun, W.; Tong, Z. Programmable and Bidirectional Bending of Soft Actuators Based on Janus Structure with Sticky Tough PAA-Clay Hydrogel. *ACS Appl. Mater. Interfaces* **2017**, *9*, 11866−11873.

(13) Chen, G.; Wen, Z.-Q.; Qiu, C.-W. Superoscillation: From Physics to Optical Applications. *Light Sci. Appl.* **2019**, *8*, No. 56.

(14) Jin, D.; Cao, J. "Perspective" - A New Approach to Serve Our Light Community. *Light Sci. Appl.* **2018**, *7*, No. 89.

(15) Li, X.; Ma, S.; Hu, J.; Ni, Y.; Lin, Z.; Yu, H. Photo-Activated Bimorph Composites of Kapton and Liquid-Crystalline Polymer Towards Biomimetic Circadian Rhythms of Albizia Julibrissin Leaves. *J. Mater. Chem. C* **2019**, *7*, 622−629.

(16) Miskin, M. Z.; Dorsey, K. J.; Bircan, B.; Han, Y.; Muller, D. A.; McEuen, P. L.; Cohen, I. Graphene-Based Bimorphs for Micron-Sized, Autonomous Origami Machines. *Proc. Natl. Acad. Sci. U.S.A.* **2018**, *115*, 466−470.

DOI: 10.1021/acsami.9b13412
ACS Appl. Mater. Interfaces 2019, 11, 37130−37138

(17) Vassalini, I.; Alessandri, I. "The Phactalysts": Carbon Nanotube/TiO_2 Composites as Phototropic Actuators for Wireless Remote Triggering of Chemical Reactions and Catalysis. *Nanoscale* **2017**, *9*, 11446−11451.
(18) Lim, H.; Park, T.; Na, J.; Park, C.; Kim, B.; Kim, E. Construction of a Photothermal Venus Flytrap from Conductive Polymer Bimorphs. *NPG Asia Mater.* **2017**, *9*, No. e399.
(19) Zha, X.; Zhang, R.-q.; Lin, Z. Tuning Thermal Expansions of Zinc Oxide Sheets by Varying the Layer Thickness. *Europhys. Lett.* **2014**, *107*, No. 26007.
(20) Wang, S.; Tambraparni, M.; Qiu, J.; Tipton, J.; Dean, D. Thermal Expansion of Graphene Composites. *Macromolecules* **2009**, *42*, 5251−5255.
(21) Yoon, D.; Son, Y.-W.; Cheong, H. Negative Thermal Expansion Coefficient of Graphene Measured by Raman Spectroscopy. *Nano Lett.* **2011**, *11*, 3227−3231.
(22) Lv, C.; Sun, X.-C.; Xia, H.; Yu, Y.-H.; Wang, G.; Cao, X.-W.; Li, S.-X.; Wang, Y.-S.; Chen, Q.-D.; Yu, Y.-D.; Sun, H.-B. Humidity-Responsive Actuation of Programmable Hydrogel Microstructures Based on 3D Printing. *Sens. Actuators, B* **2018**, *259*, 736−744.
(23) Song, Y.-y.; Liu, Y.; Jiang, H.-b.; Xue, J.-z.; Yu, Z.-p.; Li, S.-y.; Han, Z.-w.; Ren, L.-q. Janus Soft Actuators with On-Off Switchable Behaviors for Controllable Manipulation Driven by Oil. *ACS Appl. Mater. Interfaces* **2019**, *11*, 13742−13751.
(24) Wei, W.; Zhang, Z.; Wei, J.; Li, X.; Guo, J. Phototriggered Selective Actuation and Self-Oscillating in Dual-Phase Liquid Crystal Photonic Actuators. *Adv. Opt. Mater.* **2018**, *6*, No. 1800131.
(25) Han, B.; Zhang, Y.-L.; Chen, Q.-D.; Sun, H.-B. Carbon-Based Photothermal Actuators. *Adv. Funct. Mater.* **2018**, *28*, No. 1802235.
(26) Xia, D.-c.; Zhou, L.; Qiao, S.; Zhang, Y.; Tang, D.; Liu, J.; Huang, H.; Liu, Y.; Kang, Z. Graphene/Ni-Fe Layered Double-hydroxide Composite as Highly Active Electrocatalyst for Water Oxidation. *Mater. Res. Bull.* **2016**, *74*, 441−446.
(27) Jiang, H.-B.; Zhang, Y.-L.; Han, D.-D.; Xia, H.; Feng, J.; Chen, Q.-D.; Hong, Z.-R.; Sun, H.-B. Bioinspired Fabrication of Superhydrophobic Graphene Films by Two-Beam Laser Interference. *Adv. Funct. Mater.* **2014**, *24*, 4595−4602.
(28) Yu, X.; Cheng, H.; Zhang, M.; Zhao, Y.; Qu, L.; Shi, G. Graphene-Based Smart Materials. *Nat. Rev. Mater.* **2017**, *2*, No. 17046.
(29) Zhao, Y.; Song, L.; Zhang, Z.; Qu, L. Stimulus-Responsive Graphene Systems Towards Actuator Applications. *Energy Environ. Sci.* **2013**, *6*, 3520−3536.
(30) Zhang, J.; Song, L.; Zhang, Z.; Chen, N.; Qu, L. Environmentally Responsive Graphene Systems. *Small* **2014**, *10*, 2151−2164.
(31) Zhang, Y.-L.; Liu, Y.-Q.; Han, D.-D.; Ma, J.-N.; Wang, D.; Li, X.-B.; Sun, H.-B. Quantum-Confined-Superfluidics-Enabled Moisture Actuation Based on Unilaterally Structured Graphene Oxide Papers. *Adv. Mater.* **2019**, *31*, No. 1970231.
(32) Wang, W.; Zhang, Y.-L.; Han, B.; Ma, J.-N.; Wang, J.-N.; Han, D.-D.; Ma, Z.-C.; Sun, H.-B. A Complementary Strategy for Producing Moisture and Alkane Dual-Responsive Actuators Based on Graphene Oxide and PDMS Bimorph. *Sens. Actuators, B* **2019**, *290*, 133−139.
(33) Zhang, Y.-L.; Guo, L.; Xia, H.; Chen, Q.-D.; Feng, J.; Sun, H.-B. Photoreduction of Graphene Oxides: Methods, Properties, and Applications. *Adv. Opt. Mater.* **2014**, *2*, 10−28.
(34) Cheng, H.; Liu, J.; Zhao, Y.; Hu, C.; Zhang, Z.; Chen, N.; Jiang, L.; Qu, L. Graphene Fibers with Predetermined Deformation as Moisture-Triggered Actuators and Robots. *Angew. Chem., Int. Ed.* **2013**, *52*, 10482−10486.
(35) Han, D.-D.; Liu, Y.-Q.; Ma, J.-N.; Mao, J.-W.; Chen, Z.-D.; Zhang, Y.-L.; Sun, H.-B. Biomimetic Graphene Actuators Enabled by Multiresponse Graphene Oxide Paper with Pretailored Reduction Gradient. *Adv. Mater. Technol.* **2018**, *3*, No. 1800258.
(36) Zhu, L.; Gao, Y.-Y.; Han, B.; Zhang, Y.-L.; Sun, H.-B. Laser Fabrication of Graphene-Based Electrothermal Actuators Enabling Predicable Deformation. *Opt. Lett.* **2019**, *44*, 1363−1366.
(37) Vural, M.; Lei, Y.; Pena-Francesch, A.; Jung, H.; Allen, B.; Terrones, M.; Demirel, M. C. Programmable Molecular Composites of Tandem Proteins with Graphene Oxide for Efficient Bimorph Actuators. *Carbon* **2017**, *118*, 404−412.
(38) Huang, X. Y.; Brittain, W. J. Synthesis and Characterization of PMMA Nanocomposites by Suspension and Emulsion Polymerization. *Macromolecules* **2001**, *34*, 3255−3260.
(39) Han, B.; Zhang, Y.-L.; Zhu, L.; Chen, X.-H.; Ma, Z.-C.; Zhang, X.-L.; Wang, J.-N.; Wang, W.; Liu, Y.-Q.; Chen, Q.-D.; Sun, H.-B. Direct Laser Scribing of AgNPs@RGO Biochip as A Reusable SERS Sensor for DNA Detection. *Sens. Actuators, B* **2018**, *270*, 500−507.
(40) Guo, L.; Jiang, H.-B.; Shao, R.-Q.; Zhang, Y.-L.; Xie, S.-Y.; Wang, J.-N.; Li, X.-B.; Jiang, F.; Chen, Q.-D.; Zhang, T.; Sun, H.-B. Two-Beam-Laser Interference Mediated Reduction, Patterning and Nanostructuring of Graphene Oxide for the Production of A Flexible Humidity Sensing Device. *Carbon* **2012**, *50*, 1667−1673.
(41) Zhang, Y. S.; Yu, K.; Shiki, O. Y.; Luo, L. Q.; Hu, H. M.; Zhang, Q. X.; Zhu, Z. Q. Detection of Humidity Based on Quartz Crystal Microbalance Coated with ZnO Nanostructure Films. *Phys. B* **2005**, *368*, 94−99.
(42) Han, D.-D.; Zhang, Y.-L.; Liu, Y.; Liu, Y.-Q.; Jiang, H.-B.; Han, B.; Fu, X.-Y.; Ding, H.; Xu, H.-L.; Sun, H.-B. Bioinspired Graphene Actuators Prepared by Unilateral UV Irradiation of Graphene Oxide Papers. *Adv. Funct. Mater.* **2015**, *25*, 4548−4557.
(43) He, Y.; Zhu, L.; Liu, Y.; Ma, J.-N.; Han, D.-D.; Jiang, H.-B.; Han, B.; Ding, H.; Zhang, Y.-L. Femtosecond Laser Direct Writing of Flexible All-Reduced Graphene Oxide FET. *IEEE Photonics Technol. Lett.* **2016**, *28*, 1996−1999.

DOI: 10.1021/acsami.9b13412
ACS Appl. Mater. Interfaces 2019, 11, 37130−37138